Design optimization of grid-connected PV-Hydrogen for energy prosumers considering sector-coupling paradigm: Case study of a University building in Algeria

Charafeddine Mokhtara[1, 2*], Belkhir Negrou[1], Noureddine Settou[1], Abdessalem Bouferrouk[3], Yufeng Yao[3]

[1] Laboratory Valorisation et Promotion des Ressources Sahariennes (VPRS), University of Kasdi Merbah Ouargla, BP 511, 30000 4 Ouargla, Algeria.

[2] Department of Mechanical Engineering, University of Kasdi Merbah Ouargla, BP 511, 30000 4 Ouargla, Algeria.

[3] Department of Engineering Design and Mathematics, University of the West of England, Bristol BS16 1QY, U.K.

Corresponding author: Tel: +213 659 70 41 66; Email: mokhtara.chocho@gmail.com; charaf92eddine@gmail.com; mokhtara.charafeddine@univ-ouargla.dz

Design optimization of grid-connected PV-Hydrogen for energy prosumers considering sector-coupling paradigm: Case study of a University building in Algeria

Charafeddine Mokhtara[1, 2*], Belkhir Negrou[1], Noureddine Settou[1], Abdessalem Bouferrouk[3], Yufeng Yao[3]

[1] Laboratory Valorisation et Promotion des Ressources Sahariennes (VPRS), University of Kasdi Merbah Ouargla, BP 511, 30000 4 Ouargla, Algeria.

[2] Department of Mechanical Engineering, University of Kasdi Merbah Ouargla, BP 511, 30000 4 Ouargla, Algeria.

[3] Department of Engineering Design and Mathematics, University of the West of England, Bristol BS16 1QY, U.K.

Corresponding author: Tel: +213 659 70 41 66; Email: mokhtara.chocho@gmail.com; charaf92eddine@gmail.com; mokhtara.charafeddine@univ-ouargla.dz

ABSTRACT

Integrating sector coupling technologies into Hydrogen (H_2) based hybrid renewable energy systems (HRES) is a promising way to create energy prosumers, despite the very little research being done in this largely unexplored field. In this paper, a sector coupling strategy (building and transportation) is developed and applied to a grid-connected PV/battery/H_2 HRES, to maximise self-sufficiency for a University campus and to produce power and H_2 for driving electric trams in Ouargla, Algeria. A multi-objective size optimization problem is solved as a single objective problem using the ε-constraint method, in which the cost of energy (COE) is defined as the main objective function to be minimised, while both loss of power supply probability (LPSP) and non-renewable usage (NRU) are defined as constraints. Particle swarm optimization and HOMER software are employed for simulation and optimization purposes. Prior to the two scenarios investigated in this paper, a sensitivity study is performed to determine the effects of H_2 demand by trams and NRU on the techno-economic feasibility of the proposed system, followed by a new reliability factor introduced in the optimization, namely loss of H_2 supply probability (LHSP). The results of the first scenario show that by setting NRU^{max}=100%, the system without H_2 provides the best solution with COE of 0.016 \$/kWh which reaches grid parity and has 13% NRU. However, by setting NRU^{max} =1%, an optimized configuration consisting of grid/PV/Electrolyzer/Fuel cell/Storage tank is obtained, which has 0% NRU and COE of 0.1 \$/kWh. In the second scenario, it is observed that increasing the number of trams (i.e. increased H_2 demands) causes a significant reduction in LHSP, COE, NRU and CO_2 emissions. It is concluded that the grid/PV combination is the optimal choice for the studied system when considering economic aspects. However, taking into account the growing requirements of future energy systems, grid-connected PV with H_2 will be the best solution, especially when coupled with a transport system.

Keywords: Hybrid renewable energy systems; Grid-connected PV system; Hydrogen economy; Building-transportation sector coupling; Size optimization; Energy prosumers.

Abbreviations

AC	Alternative Current
CO$_2$	Carbon Dioxide
COE	Cost of Energy
DC	Direct Current
Ele	Electrolyzer
FC	Fuel Cell
GA	Genetic Algorithm
GHG	Greenhouse Gas
H$_2$	Hydrogen
HRES	Hybrid Renewable Energy System
LHSP	Loss of Hydrogen Supply Probability
LPSP	Loss of Power Supply Probability
NOCT	Nominal Operation Cell Temperature
NRU	Non-Renewable Usage
PEM	Proton Exchange Membrane
PSO	Particle Swarm Optimization
PV	Photovoltaic
RU	Renewable Usage
ST	Storage Tank
WT	Wind Turbine

1. Introduction

In recent decades, buildings and transportation sectors have caused a massive energy and environmental burden owing to their large dependency on fossil fuels. According to published reports, about 80% of the world's primary energy supply [1], and 97% of the total energy provided in Algeria [2] are fossil fuel based. About one-third of the global greenhouse gas (GHG) emissions come from the building sector which consumes more than 40% of the global electricity production [3,4]. This is mainly due to the increase in the number of consumers and energy-intensive high living standards. Thus, the electricity sector currently faces two major but seemingly contradicting challenges, i.e. maintaining a sufficient supply to meet the ever-increasing demand for electricity, and reducing CO$_2$ emissions [5].

In response to these issues, many countries and international organizations have established various energy policies. Besides, numerous research works are being conducted across the globe to find better and environmentally-friendly solutions that could meet present and future energy demands. One possible solution is to integrate building energy supplier system with localized renewable sources such as roof-mounted solar photovoltaic (PV). Recently, owing to the significant reduction in PV panels' investment cost, enhanced efficiency, and faster and easier integration onto the buildings' off-print (e.g. roofs), there has been an increased trend in implementation of PV systems worldwide. Algeria has a large solar energy potential, mainly in the Sahara region [6], and thus the government's new vision is to increase its renewable energy share up to 27% of total energy supply by 2030 [7]. However, power generation by PV panels is weather dependent and it is only active during the daytime. Hence, combining PV with existing fuel-based sources to make a hybrid renewable energy systems (HRES) together with an energy storage unit, provides a promising solution for increasing system reliability, reducing CO$_2$ emissions and energy costs. The potential benefits of such a hybrid solution can be further multiplied if used to produce clean fuels such as renewable hydrogen (H$_2$), e.g. from solar powered electrolysis. Hydrogen can then be used in fuel cells to produce electricity for transportation. This HRES-H$_2$ combination offers

opportunities to investigate system optimization in terms of many factors including size, energy usage, costs, CO_2 emissions and reliability.

1.2 Bibliometric analysis and literature review

Many studies in the literature have investigated the size optimization of HRES. To identify the most frequently used factors, criteria, and optimization techniques, a bibliometric analysis is firstly performed by the authors (to the authors' knowledge, such an analysis has not previously been applied in the HRES research field), focusing on hydrogen based HRES (H_2-HRES), which is the main focus of this study. Besides, this analysis is useful to construct the literature review section and quickly identify the shortcomings in previous works by searching for a few keywords such as "hybrid renewable energy system" and "size optimization" in Elsevier publication database over the last decade (from 2010 to 2020). Despite the limitation of accessing resources, the Elsevier database is adequate and the proposed methodology is applicable to other databases such as Springer and IEEE. Using the VOSviewer tool [8,9], the search results can be visualized and presented in a network map and as well as an overlay map, shown in Fig. 1 and Fig. 2, respectively.

Fig. 1. Network visualisation for the most used words (in papers' title, indexed keywords and abstract). Note: the most used words are classified into four clusters identified by colours. Each cluster includes words that belong to a particular topic (**Blue cluster**: represents the function in the technical optimization of HRES using AI algorithms; **Green cluster**: represents the economic optimization of HRES using Homer; **Yellow cluster**: represents the main topics related to renewable energy based systems; **Red cluster**: represents the effect of H_2 storage integration on the performance of HRES).

Fig. 2. Overlay visualisation for the most used words (in papers' title, indexed keywords, and abstract; the clusters here are divided based on the year of publication. For example, **Purple cluster**: shows that before 2016, researchers are more interested in the optimization of off-grid HRES using Homer; **Yellow cluster**: shows that recently (from 2017 up to now), there has been an increased interest by researchers in grid-connected H_2 based HRES using AI algorithms.

From the network visualisation map (Fig.1), these bibliometric analyses show that the majority of researchers have focused on meeting the demand of the building energy usage by increasing the self-sufficiency while improving the system reliability (e.g. indicated by keywords such as the loss of power supply probability, LSLP) and reducing the overall system cost (e.g. indicated by keywords such as the cost of energy, COE and the net present cost, NPC). Also, the problem of size optimization in HRES can be solved in general by simulation approaches using software tools (such as HOMER) or optimization algorithms, including classical methods and/or advanced artificial intelligence (AI) techniques (such as particle swarm optimization, PSO and genetic algorithm, GA) [10], as indicated in both the overlay and the network maps.

The following is a summary of some major recent works in the field of size optimization and economic viability of HRES. In [11], Hou et al. optimized the size of a hybrid wind turbine (WT)/PV/Storage energy system. Design optimization of an off-grid HRES for rural isolated areas was undertaken by Aberilla et al. [12]. In [13], Cai et al. carried out the size optimization and economic evaluation of an off-grid PV/Battery/Diesel HRES. In [14], Modarresi et al. developed a heuristic optimization algorithm for determining the optimal size of an off-grid hybrid PV/Battery/Diesel energy system, considering vehicle to grid (V2G) technology. The optimal design of a hybrid PV/Battery energy system for a University campus under an unreliable grid connection was conducted by Chedid et al. [15]. In [16], Li et al. studied the effects of battery technology selection on the technical and economic performance of WT/Diesel/Battery off-grid hybrid energy systems. In [17], Ashraf et al. optimized the size for an off-grid PV/diesel/battery hybrid energy system using a metaheuristic algorithm. In [18], Xu et al. optimized the sizing of an isolated PV/WT/Hydropower/Storage HRES using multi-objective particle swarm optimization (MOPSO). In [19], Berbaoui et al. applied a methodology for the size optimization of a HRES for an isolated area in Algeria using virus colony search algorithm. In [20], Alshammari et al. used harmony search, Jaya and particle swarm optimization algorithms for optimal sizing of HRES, consisting of PV/WT/Battery/Biomass generators. The techno-economic assessment and optimal size of grid-connected PV/wind/diesel/storage HRES was also undertaken by Dahiru et al. [21] for tropical climates. Multi-objective genetic algorithm for the design optimization of a small-scale PV/WT/Solar heat collector/Heat pump/Heat and power storage HRES was carried out previously [22]. In [23], Habib et al. used artificial bee colony (ABC) optimization to perform a multi-objective optimization

5

of HRES, considering V2G technology. Nguyen et al. [24] conducted an optimal sizing of an HRES, based on multi-objective decision-making algorithm to provide the necessary energy demand of a wastewater treatment plant. In [25], Jaszczur et al. used multi-objective algorithm (NSGA-II) for the design optimization of an HRES in the household application. In [26], Wang et al. conducted multi-objective optimization for PV/WT/Battery/Diesel HRES. Most recently, Mokhtara et al. [27] developed an efficient energy management strategy for optimal design and operation of a HES for electrification of residential buildings in rural areas of Algeria.

Due to the emergence of renewable H_2 (i.e. the production of H_2 from renewable sources such as solar powered electrolysis) to serve as an alternative fuel for future energy systems [28], the increasing popularity of fuel cell (FC) vehicles [29], and the ability of modern batteries to provide long-term and large-scale storage solutions, H_2-HRES systems have recently (i.e. 2017 onwards, see Fig. 2) gained an increasing interest from researchers worldwide [30]. For the integration of H_2 in HRES within building environments, there are various methods in the literature that have already been investigated. The remaining challenge is to explore any promising options that can not only satisfy building energy requirements and enable building operations to reach high self-sufficiency, but also act as a key ingredient in creating energy Prosumers. This can be achieved by performing power and H_2 exchange with other users via sector coupling technologies (such as the power import from or export to the electricity grid or their neighbouring buildings [31], and H_2 import from or export to transportation and manufacturing sectors, respectively). Converting surplus electricity into H_2 and exporting it for use in the transport sector is one such option that could enable the promotion of renewable energy, energy conservation and the reduction of the dependency on fossil fuels. The H_2 is considered by many as the green fuel for future electric vehicles and producing H_2 from HRES can be very promising for sustainable future energy systems. Nevertheless, the design optimization and techno-economic feasibility analysis of such complex systems is highly challenging, particularly in relation to the presence of different types of energy sources (i.e. electricity and H_2).

The following section summarises some noticeable recent studies related to optimization of an off-grid HRES when integrated with H_2 storage. Duman et al. [32] used HOMER software to carry out the techno-economic analysis of an off-grid PV/WT/FC HRES considering two household occupancy scenarios: seasonal and regular. They also compared between hydrogen and battery storage under different values of renewable fraction (RN). Zhang et al. [33] carried out the optimization of an HRES that includes battery and H_2 storage based on simulated annealing (SA) algorithm. In addition, they compared their algorithm with hybrid harmony search to further evaluate its performance. Mohamad et al. [34] used a flower pollination algorithm to optimize a PV/FC HRES to supply remote off-grid areas in Egypt. Furthermore, the impact of the variation of the initial cost of components on the COE is evaluated based on a sensitivity analysis. Jamshidi et al. [35] used multi-objective crow search algorithm to perform the techno-economic optimization of a PV/FC/diesel HRES for an off-grid community in Iran. Here, the authors took into account the effects of the uncertainties of load and operating reserve on the optimal size of the system. A thermo-economic analysis was performed by Jafari et al. [36] to optimize a stand-alone solar/H_2/battery HRES. The proposed system is optimized to meet an annual electricity and heating demand of buildings under off-grid operation. Mohamad et al. [37] performed a techno-economic optimization of a solar PV/WT/FC HRES for a small-scale application in Egypt using the firefly algorithm. The aim of that study was to increase the share of renewable energy and to investigate the possibility of using H_2 storage system as an alternative to batteries. Zhang et al. [38] performed a size optimization of a stand-alone PV/WT/H_2 HRES using a hybrid search optimization algorithm, in which the authors integrated a weather forecasting model into the optimization to increase the accuracy of the sized system. Ghenai et al. [39] undertook the size optimization and techno-economic evaluation of an off-grid PV/FC HRES for a residential community in a desert area. Mokhtara et al. [40] used HOMER tool and performed an analytical hierarchy process for the optimal design of an off-grid hybrid PV/WT/Diesel/Battery/H_2 energy system for the electrification of mobile buildings in Algeria. In their study, they investigated many configurations of the proposed system taking into account the effects of fuel cost. In [41], Firtina et al. performed the size optimization of an off-grid hybrid wind/H_2 system for achieving zero-energy building in an isolated area in Turkey. Their study showed that small timeframes (10 minutes) of time step of climate data was crucial to ensure high system reliability. In [42], Zhang et al. used an efficient heuristic approach for the optimal size of an off-grid PV/H_2 system for rural locations. The components sizing of an off-grid WT/H_2/Battery/Super-capacitor HRES was carried out by Attemene et al. [43]. In [44], Haddad et al. implemented

a performance comparison between two solar/FC hybrid energy systems for a case study in a Lebanese city. Xu et al. [45] performed the size optimization of an off-grid WT/PV/H_2 system based on a modified NSGA-II algorithm and a multi-criteria decision making technique. The proposed system was optimized to meet an off-grid industrial park's load demand in China. Design optimization of an off-grid H_2-HRES for electrification of remote areas was studied by Suresh et al. [46], who used both GA and HOMER software to obtain the optimal configuration of their HRES with reduced costs and CO_2 emissions. Gutierrez-Martín et al. [47] presented a methodology for optimal design of PV/H_2 HRES taking into account the effects of climate data and the components characteristics. The objective of their work was to ensure the load needs were met at an acceptable cost. Abadlia et al. [48] applied a fuzzy controller with genetic algorithms for design optimization of grid-connected PV/H_2 HRES to ensure high performance power generation systems. Saleem et al. [49] used TRNSYS to achieve optimal design of a hybrid PV/H_2/battery energy system under two different climates. Haddad et al. [50] optimized a hybrid wind/PV/FC energy to reduce the effects of energy shortage during some periods using a case study region in Lebanon. Lin et al. [51] examined a grid-connected hybrid PV/H_2 in case of reactive power management, in order to improve the reliability of power supply system. They used genetic algorithm to select the site for hosting the proposed HRES with optimized cost. Maghami et al. [52] developed an energy management strategy based on demand response and integrated with a H_2 based HRES to reduce the peak demand, minimize costs and enhance battery lifespan. Lokar and Virti [53] investigated the ability of integrating H_2/PV/battery HRES to ensure high self-sufficiency in residential buildings in a pilot study building located in Slovenia. You et al. [54] studied the socio-economic and environmental impacts of a hybrid H2/wind/natural gas supply system for the transport sector, from production to final distribution (e.g. fueling stations). Kamel et al. [55] applied a hybrid energy management strategy for enhancing the operation of FC/PV/battery/supercapacitor HRES. Marocco et al. [56] analyzed the techno-economic and environmental feasibility of HRES with H_2 storage for supplying remote areas in Europe. Gu et al. [57] carried out a comparative study for the techno-economic feasibility of PV/H_2 HRES for supplying hydrogen refueling stations in China. Ghaffari et al. [58] presented an efficient optimization approach based on a modified version of crow search algorithm (CSA) for size optimization of a hybrid PV/diesel/FC energy system, in which NPC is minimized subject to two main constraints: LPSP and RF. Rad [59] performed a techno-economic analysis of a H_2 based HRES for the cost-effective rural electrification in Iran.

Despite these extensive works for off-grid applications, there is a growing trend of applying some innovative grid integration technologies, including V2G, power to gas, and FC tram in order to facilitate sector coupling [60]. Unfortunately, until now, there have been limited publications on the design of grid-connected HRES, especially those incorporating H_2 storage. Tebibel et al. [61] presented a comparative performance analysis of grid-connected PV/H_2 production using water, methanol, and hybrid sulphur electrolysis processes. In addition, the effect of each type of electrolysis on the size of the proposed system was evaluated. In [62], Gharibi et al. implemented a multi-objective crow search algorithm for size and power exchange optimization of a grid-connected Diesel/PV/FC hybrid energy system considering reliability, cost, and renewable energy consumption. Similarly, García et al. [63] used a multi-objective PSO for optimal operation of a grid-connected WT/PV system with hybrid battery/H_2 storage. Singh et al. [64] developed a hybrid ABC-PSO algorithm for optimal sizing of a grid connected PV/FC energy system. The system was designed to supply the electricity demand of a small shop at a University campus in India. Both the cost of energy purchased from and sold to the grid were considered in the optimization. Darras et al. [65] performed the economic optimization of a grid-connected PV/H_2 system to meet the required power demand with low-cost of injection-to-grid, where the authors used ORIENTE® software to determine the optimal size of components.

According to the aforementioned literature, the majority of papers have focused on the design of off-grid HRES's and only a few papers have considered grid-connected applications. The advantages of previously published works are the application of diverse optimization algorithms, the use of multiple renewable energy sources, and integrating H_2 storage systems efficiently to meet the energy demand of buildings particularly in remote areas where it is difficult to connect to the electricity grid. However, studies on HRES-H_2 that consider the interconnection between buildings and other sectors such as transport have not been widely conducted.

In this study, a new approach to mitigate CO_2 emission by providing power and renewable H_2 from solar energy to supply buildings and public transportation is introduced. The proposed HRES-H_2 system uses solar PV to power

a University campus building, and converts the surplus power to H$_2$ via proton exchange membrane (PEM) Electrolyzer (Ele) which is then used to supply electric trams in the city of Ouargla, Algeria. The proposed PV/H$_2$ HRES is investigated in a grid-connected topology, since 99% of buildings in Algeria are connected to the electricity grid [3]. The objective of this study is to optimally size the proposed HRES to meet the load demands of the selected building. In turn, this would reduce the imported power from the grid (by increasing building self-sufficiency), reduce the cost of energy (by reaching grid parity), as well as decreasing the peak loads limit. The novelty of this work is to interconnect building energy systems with the public transportation sector (via electric-powered trams) to increase the share of renewable energy and make it feasible from the technical, economic, and environmental viewpoints. Of course there are other studies that have looked into building/transport coupling for HRES-H$_2$, however, to the authors' best knowledge no study has yet been proposed to integrate large scale buildings to public means of transportation. To achieve these goals, the following tasks are undertaken: (1) search and determine the optimal sizing of the proposed grid-connected hybrid PV/H$_2$ system via sensitivity analysis; (2) perform techno-economic feasibility study of energy prosumers in Algeria (Ouargla as a case study); (3) quantify the effect of integrating a sector coupling strategy (by exporting and selling the produced H$_2$ to charge the FC based trams) on the size optimization of a grid-connected HRES. The remaining parts of this paper are devoted to the presentation of the problem to be solved, the methodology adopted, and the results obtained with discussions. Finally, the key findings, conclusions and future recommendations are outlined.

2. Problem definition and mathematical modelling

The HRES-H$_2$ under study includes PV panels, FC, Ele, H$_2$ storage tanks (STs), electricity grid and an inverter, as presented in Fig. 3. In contrast to some previous works which focused on off-grid applications, here the HRES is optimized under grid-connected topology. The energy management system applied for the operation of this HRES will be discussed later in the simulation section. A description of the system components and mathematical modelling is as follows.
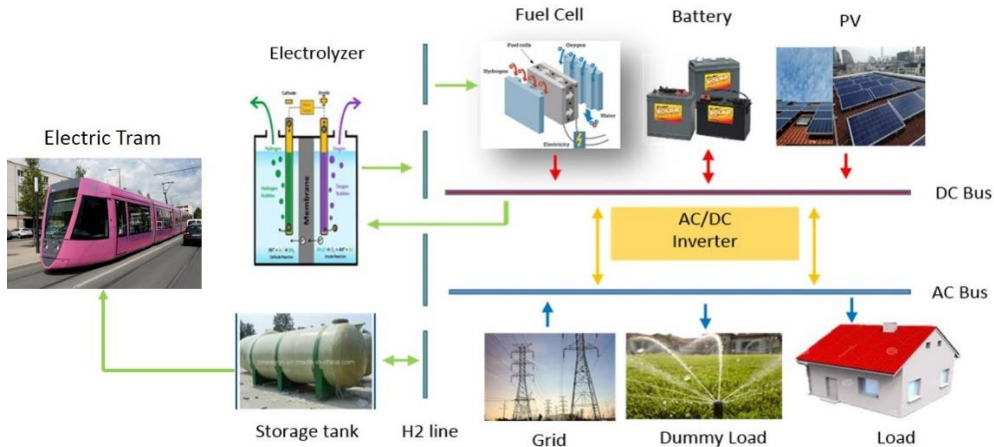
Fig. 3. Schematic of the studied grid-connected PV/H$_2$ hybrid system.

2.1 Solar photovoltaic

The electric output power of a PV module is evaluated using eq. 1 [66]

$$P_{pv} = P_{Npv} \times \frac{G}{G_{STC}} \times \left[1 + K_t \times \left(\left[T_{amb} + \frac{NOCT - 20}{800}\right] \times G - T_{STC}\right)\right] \qquad (1)$$

where P_{pv} and P_{Npv} are the output power and rated power of the PV module (in kW), respectively. The parameters G and T_{amb} are the solar radiation (kW/m²) and ambient temperature (°C) during a simulation time step, whereas G_{STC} (1 kW/m²) and T_{STC} (25°C) are solar radiation and ambient temperature at standard conditions. K_t is

the temperature coefficient of power (-0.41 %/°C), which depends on PV's panel technology, and is related to nominal operation cell temperature (NOCT in °C).

2.2 H₂ system

This system includes three parts: the Ele, ST, and FC. A simplified FC and Ele models are used in this study. However, it is assumed that the FC and Ele work at an operation point which depends on the energy generated and energy demand at a simulation time, t. Similarly, the size of the ST needs further analysis inclusive of the Ele, FC, total energy generated and energy demand requirements. When the generated energy Eg (t) ≥ the energy demand E_l (t), the surplus electricity is used to produce H_2 gas by using the Ele. The produced H_2 is then stored in a hydrogen ST. The charge of ST is calculated using eq. 2 [38]. However, when Eg (t) ≤ E_l (t), FC is used to supply the rest of the power load. In this case, the charge of ST is calculated using eq. 3 [38]. When the FC cannot meet the required load, or if there is no FC in the system, the building will import the required electricity from the grid.

$$ST(t) = ST(t-1) + \left(E_g(t) - \frac{E_l(t)}{\eta_{inv}}\right) \times \eta_{Ele} \qquad (2)$$

$$ST(t) = ST(t-1) - \left(\frac{E_l(t)}{\eta_{inv}} - E_g(t)\right) / \eta_{FC} \qquad (3)$$

where $ST(t)$ and $ST(t-1)$ are the energy stored (kWh) in the ST at times (in hours) of t and $t-1$, respectively. The charge of ST has a maximum limit (ST_{max}), which represents the capacity of ST. The parameters η_{Ele} and η_{FC} are the efficiency of Ele (90%) and FC (50%), respectively [37] while η_{inv} is the power inverter efficiency as defined in eq. 4 below.

2.3 Grid

When the PV system and storage devices are not sufficient to supply the required loads, the grid is used to supply the deficit energy. In Algeria, the purchase price rate (PPR) for the electricity is 0.05 $/kWh. In case of availability of export electricity to the grid, the sell price rate (SPR) for the electricity is assumed to be the same as PPR (i.e. 0.05 $/kWh). The CO_2 emission is evaluated according to the imported energy from the grid. It is assumed that the CO_2 emitted by one kWh electricity from the grid is 0.632 $/kWh (i.e., a standard value from HOMER software).

2.4 Inverter

The power inverter is an electric device used for converting electricity from direct current (DC) produced by PV modules or generated from FCs to alternate current (AC) to operate building loads. The size of the inverter is a function of the inverter efficiency η_{inv}, defined in eq. 4, and input and output power to/from the inverter:

$$\eta_{inv} = \frac{P_{output}(t)}{P_{input}(t)} \qquad (4)$$

2.5 Load profile and climate data

The studied educational building, located in a hot dry climate, has a total roof area of 18209 m² and has an energy demand of 1486 MWh/year. Fig. 4 shows a map of the building and its geographic location (from Google Earth), including its proximity to the tramway line. Besides, the load profile of the campus (as supplied by the national electricity supplier Sonelgaz) is presented in Fig. 5. Meteonorm 7 software is used to collect the climate data for the building location. Fig. 6 and Fig. 7 illustrate the total radiation and hourly ambient temperature at the building location (Ouargla, Algeria), respectively.

9

Fig. 4. University campus location and tramway line in Ouargla, Algeria.
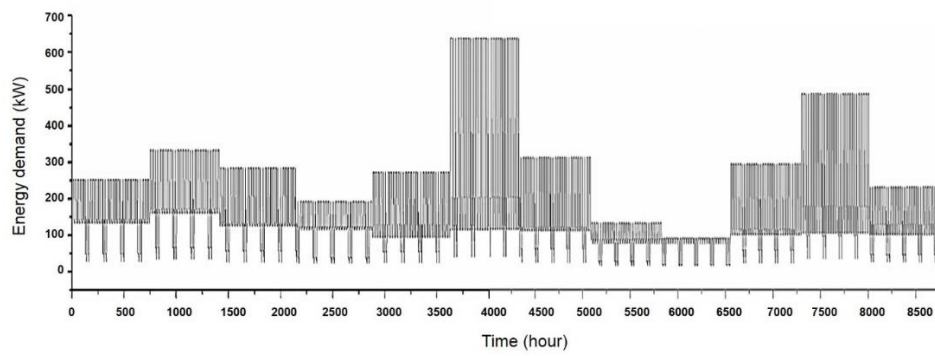
Fig. 5. Campus building's yearly load profile (considering five working days in a week).
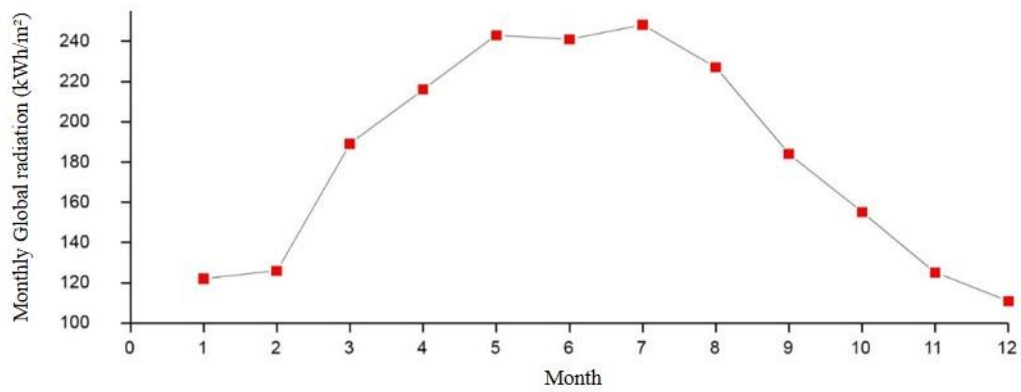
Fig. 6. Monthly total radiation at the campus building location (Ouargla, Algeria).

10
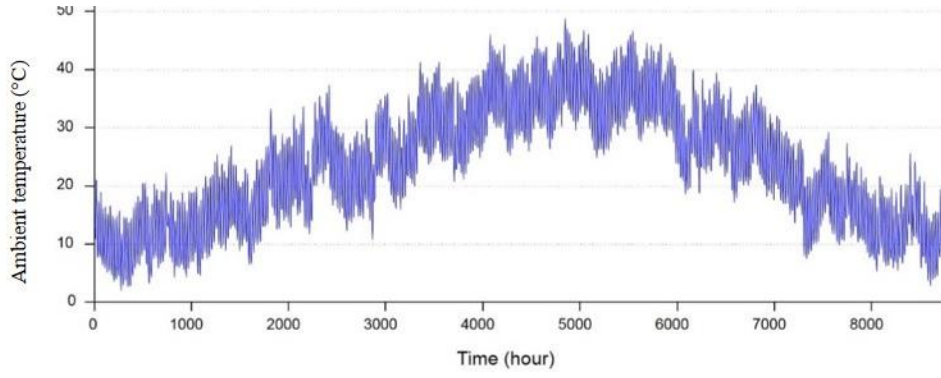
Fig. 7. Hourly ambient temperature at the building location over one year (Ouargla, Algeria).

3. Formulation of the multi-objective problem

A multi-objective problem could be defined as optimising multi-purpose goals while meeting all constraints by identifying the variables of the decision [67]. In this work, the multi-objective problem consists of four objectives to be minimized: the cost of energy (COE), loss of power supply probability (LPSP), loss of H_2 supply probability (LHSP), and non-renewable usage (NRU).

3.1 Objective functions

3.1.1 Cost of energy
This parameter is widely used to evaluate the economic feasibility of HRES. The COE for a grid-connected system can be calculated using eqs. 4-12 [25, 32–34].

$$COE(\$/KWh) = \frac{C_{A\_cap} + C_{A\_O\&M} + C_{A\_rep} + C_{Grid\_P} - C_{H_2} - C_{Grid\_S}}{E_{served} + H_{2\,served}} \tag{5}$$

$$C_{A\_cap}(\$) = (P_{Npv} \cdot C_{PV} + P_{Cnv} \cdot C_{Cnv} + P_{FC} \cdot C_{FC} + P_{Ele} \cdot C_{Ele} + ST_{max} \cdot C_{ST}) \times CRF \tag{6}$$

$$C_{A\_O\&M}(\$) = 0.02 \times C_{A\_cap} \times \sum_{k=1}^{T} \frac{1}{(1+j)^k} \tag{7}$$

$$C_{A\_rep}(\$) = FC \times C_{FC} \times \sum_{k=10}^{T} \frac{1}{(1+j)^k} \times CRF \tag{8}$$

$$CRF = \frac{i(1+i)^T}{(1+i)^T - 1} \tag{9}$$

$$C_{Grid\_P} = EPR \times E_{Grid\_P} \tag{10}$$

$$C_{Grid\_S} = SPR \times E_{Grid\_S} \tag{11}$$

11

$$C_{H2} = SH_2 \times H_{2S} \qquad (12)$$

where E_{Grid_P}, E_{Grid_S}, and H_{2S} are the energy purchased from the grid, the energy sold to the grid and the amount of H_2 sold to the grid, respectively. C_{Grid_P}, C_{Grid_S}, and C_{H2} are the cost of energy purchased from the grid, the cost of energy sold to the grid and the cost of H_2 sold, respectively. CRF is the capacity recovery factor, while T and i are the project lifetime (in years) and the real interest rate, respectively. C_{PV}, C_{inv}, C_{FC}, C_{Ele}, and C_{ST} are the capital investment cost for the PV, inverter, FC, Ele, and ST, respectively. C_{A_cap}, $C_{A\_O\&M}$, and C_{A_rep} are respectively the annual capital investment cost, operation, and maintenance cost and replacement cost. P_{Npv}, P_{inv}, P_{FC}, and P_{Ele} are the rated capacities of the PV, inverter, FC and Ele, respectively. In this study, the H_2 sell rate (SH$_2$) is set at 3.3 \$/kg (i.e. 0.08 \$/kWh) [71], similar to the sell rate of hydrogen gas produced by natural gas.

3.1.2 Loss of power supply probability

LPSP represents the ratio of the annual energy that the HRES fails to meet to the annual required demand of the building. Hence, this function must be minimized to increase the system reliability. LPSP is assessed based on eq. 13 [27].

$$LPSP(\%) = \frac{\sum_0^T E_l(t) - P_{pv}(t) - E_{Grid\_P}(t) - FC_{prov}(t)}{\sum_0^T E_l(t)} \qquad (13)$$

where FC_{prov} is the energy that can be provided by FC. The LPSP value is in the range of [0, 1].

3.1.3 Loss of hydrogen supply probability

LHSP index introduced in this study represents the sum of the amount of H_2 which is unable to meet demand ($H_{2\text{-unmet}}$) divided by the total required H_2 ($H_{2\text{-req}}$), considering the number of trams to be charged (on an annual basis), as defined by eq. 14, to ensure the amount of H_2 required by trams is being met. Similar to LPSP, the LHSP is in the range of [0, 1].

$$LHSP(\%) = \frac{\sum_0^T H_{2-unmet}(t)}{\sum_0^T H_{2-req}(t)} \qquad (14)$$

3.1.4 Non-Renewable Usage

NRU is defined as a ratio of fossil fuel usage divided by the sum of the total energy provided (including energy from renewable and non-renewable sources). NRU can be calculated using eq. 15. Hence, renewable usage (RU) that represents the contribution of renewable sources for the supply of load demand is evaluated using eq. 16.

$$NRU(\%) = \frac{E_{Grid\_P}}{E_{Grid\_P} + E_{pv}} \qquad (15)$$

$$RU(\%) = 1 - NRU \qquad (16)$$

where E_{Grid_P} and E_{pv} are the total energy purchased from the grid and the total generated energy from the PV system, respectively. Similarly, NRU is in the range of [0, 1].

3.2 Optimization problem formulation

To reduce the time of calculation and decision making during the selection process of the best solution among a set of possible solutions from the Pareto optimal solution set, a classical method to solve the multi-objective problem is implicitly used. In this approach, the ε-constraint method [72] was used to reformulate the problem in one main objective (i.e. minimising COE) whilst the other three objectives (i.e. minimising LPSP, LHSP and

NRU) are defined as constraints. In addition, four persistent decision parameters of PV panels, Ele, STs and FCs must also be determined. The main objective function Z is defined in eq. 17.

$$Z = \min \cdot COE(N_{PV}, N_{Ele}, N_{FC}, N_{ST}),\qquad(17)$$

where N_{PV}, N_{Ele}, N_{FC}, N_{ST} are the size of PV, Ele, FC and ST, respectively, subject to the decision variable constraints of eqs. 18, 19 and 20:

$$0 \leq LPSP \leq LPSP^{max} \qquad \text{and} \qquad 0 \leq LHSP \leq LHSP^{max}\qquad(18)$$

$$0 \leq NRU \leq NRU^{max}\qquad(19)$$

$$0 \leq N_{PV}, N_{Ele}, N_{FC}, N_{ST} \leq N_{PV}^{max}, N_{Ele}^{max}, N_{FC}^{max}, N_{ST}^{max}\qquad(20)$$

3.3 Design optimization via particle swarm optimization

PSO is considered to be the most frequently used method of artificial intelligence in the optimization of HRES [73]. PSO is a metaheuristic optimization technique inspired firstly by general artificial life [74]. In PSO, a set of particles (also known as 'swarm'), defined by their positions and velocity vectors, move through the search space, seeking to reach their local best and global best for the swarm. The main steps in PSO to find the global best solution for a given optimization problem are as follows.

3.3.1 Step 1: Initialization of PSO parameters

Parameters of the PSO used in this work are given in Table 1 [34].

Table 1. Parameters of the PSO.

Parameter	Value
Maximum number of iterations	55
Population Size	25
The dimension of the search variables	4
Intertie Weight Damping Rate	0.9
Weight of Inertia	0.8
Coefficient of Personal Learning	1.8
Coefficient of Global Learning	1.95

3.3.2 Step 2: Initialization of particles' position, local and global optimum

In this step, the initialization of particle velocities and positions for all populations is performed by setting random values, and then evaluating the fitness of each particle. Thus, the best value for the initial population is determined (i.e. minimum COE in this work). In addition, the maximum values for the constraints (LPSP, LHSP and NRU) and limit boundaries for decision variables are introduced. Here, the upper bound for the PV capacity is 1916 kW (based on the total roof area and the required area for one kW of PV modules). As there are no boundary limits for the other decision variables, large values for their upper bounds are set.

3.3.3 Step 3: Update the position of particles

The position and velocity of each particle in the swarm is updated at the (k+1) iteration time step using the recursive eqs. 21 and eq. 22 [75], respectively.

$$X_{k+1}^i = X_k^i + v_{k+1}^i\qquad(21)$$

$$v_{k+1}^i = [\omega v_k^i + C_1 r_1(P_k^i - X_k^i) + C_2 r_2(P_k^g - X_k^i)] \tag{22}$$

Where, $v_k^i\ and\ v_{k+1}^i$ represent the particle velocity at the actual and next iteration, respectively. The term $C_1 r_1(P_k^i - X_k^i)$ is called the cognitive component, and causes the particle to return to a previous position in which it has experienced higher individual fitness. $C_2 r_2(P_k^g - X_k^i)$, is called the social component, P_k^i is the best individual particle position and P_k^g is the best global position, C_1 and C_2 are personal (cognitive) and global (social) learning coefficients, respectively; r_1 and r_2 are random numbers between 0 and 1, ω is a coefficient. The parameters of the PSO algorithm used in this work are taken from a published work [76].

3.3.4 Step 4: Determine the best solution and optimal size of components

Based on the updated values of particles' positions, and after performing a certain number of iterations (as defined by the user), the final value of the global best (the best solution) is determined. Hence, the value of decision variables (that represent the size of HRES's components) is evaluated accordingly. The pseudo-code for the PSO algorithm is given in Fig. 8.

```
For each particle
    initialize particle (random values)
End (For)

While maximum iterations or minimum error criteria is not attained, Do

 For each particle
    Calculate fitness value
    If the fitness value is better than the best fitness value P_k^i  in history
        Set current value as the new P_k^i
    End (If)
    Choose the particle with the best fitness value of all the particles the P_k^g
        For each particle
        Calculate particle velocity according to the following equation
        v_{k+1}^i = [ωv_k^i + C_1 r_1(P_k^i − X_k^i) + C_2 r_2(P_k^g − X_k^i)]
        Update particle position according to the following equation
                X_{k+1}^i = X_k^i + v_{k+1}^i
        End For

End (While)
```

Fig. 8. The pseudo-code of the PSO algorithm.

4. Simulation scenarios

Here, a structure for the optimization of grid-connected PV/H$_2$ hybrid schemes to meet the power load of a building as well as supplying a neighbouring electric tram in the case study location is implemented (Fig. 9). Two energy management strategies are established first for optimizing the energy flow between the components of the investigated grid-connected HRES. Then, PSO method is used to determine the optimal size of components that leads to the reduced COE, and increased system reliability under specified renewable energy usage, depending on the chosen simulation scenarios (SS) and the applied energy management strategy. The description of the energy management strategy that is adopted to optimize the grid-connected PV/H$_2$ hybrid system is given as follows, according to each scenario.
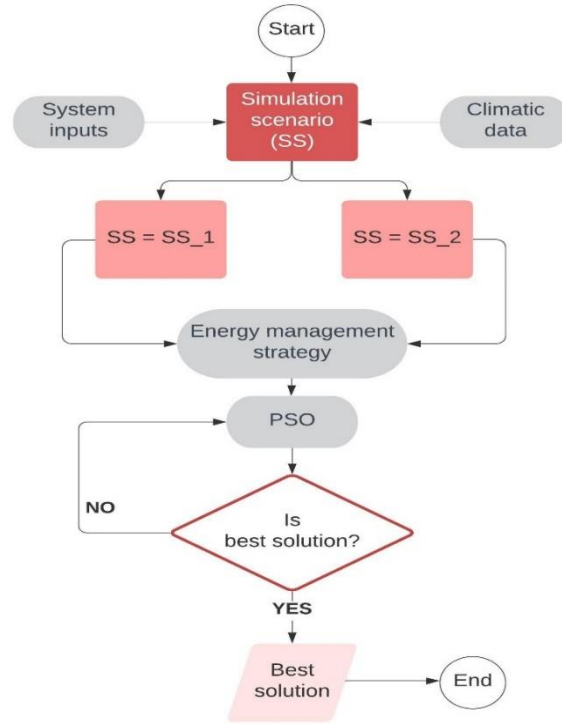
Fig. 9. The block diagram for the proposed optimization framework with two simulation scenarios.

4.1 Scenario 1

In this scenario, the investigated HRES consists of a grid-connected PV system, Ele, FC and H_2 ST. Here, both export to and import from the grid are allowed. However, the sale of H_2 is not included (as sector coupling is not applied in this scenario). The system is optimized through a sensitivity analysis, in which the value of NRU^{max} is varied between 1% (the first case) and 100% (the second case).

Energy management strategy (Scenario 1)

In this scenario, the PV system is the first source used to supply the building demand. When the produced electricity by PV is more than the energy demand, the surplus electricity is used to produce H_2 by the Ele and then it is stored in the ST. If further surplus exists, the excess electricity is exported to the grid. On the another hand, when the produced electricity by PV is less than the energy demand, in this case, the FC is used for meeting the required demand. However, if the FC cannot provide the required demand (e.g. either a shortage in H_2 or the maximum FC capacity is insufficient) the grid must provide the remaining demand. In case of any shortage, the LPSP is evaluated. A flow chart for the energy management strategy applied in scenario 1 is detailed in Fig. 10.

4.2 Scenario 2

In this scenario, the investigated HRES consists of a grid-connected PV system, Ele, and H_2 ST. Here, export of electricity to the grid is not considered. However, the building can import electricity when the purchased electricity rate is similar to that used in the first scenario (0.05 $/kWh). In this scenario 2, a sector coupling strategy (building-transportation sectors) is proposed by integrating an onsite H_2 refuelling station, in which the produced H_2 by the building is exported to the refuelling station for charging a hybrid FC tramway [77]. In the city of Ouargla, where the University campus is located, there is a city tramway (50 m away from the campus main gate) as shown in Fig. 11. The tramway has been in operation since 2018, and drives along a 10 km tramline section (including 16 stops) and operates 7/7 days, from 05:00 to 23:00 each day [78].

15
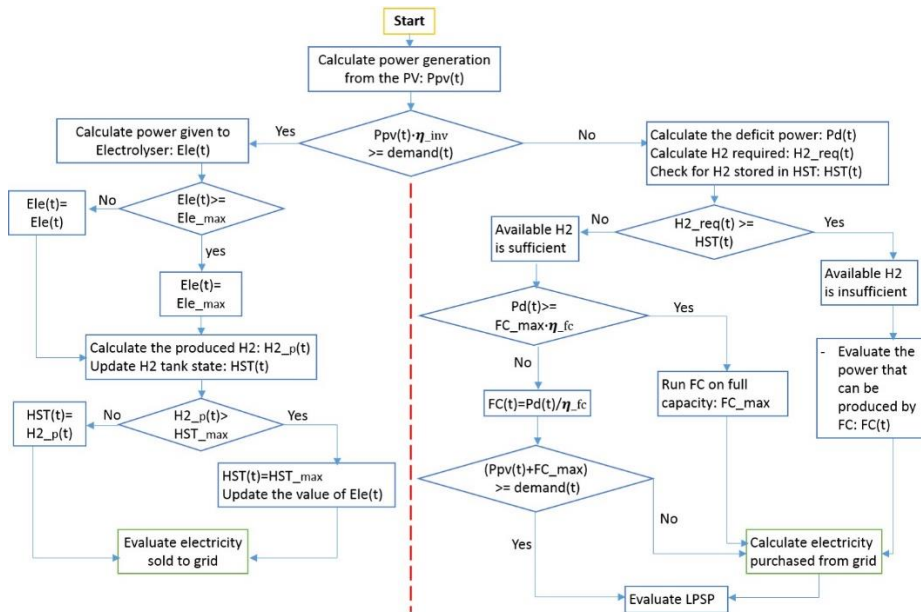
Fig. 10. Schematic of the studied grid-connected PV-H₂ hybrid system without sector coupling strategy (Scenario 1).

Hence, the trams are operational for 15 h/day (excluding stops). There are eight trams, of which four are still in operation and four are in standby. Therefore, the maximum number of trams that consume energy every day is four. It is assumed that the required H_2 for the operation of a single tram running at 20-25 km/h is 16.5 kg/100 km [79]. Thus, the average speed of the studied trams is 20 km/h, accounting for 15h of operation per day, and the daily total distance that can be achieved by one tram is 300 km. Hence, the required H_2 for each tram would be 50 kg/day (or equivalent to 1665 kWh, as 1 kg H_2 contains 33.3 kWh). The fuel cell trams can also operate with electricity (from electricity line or from batteries). In hybrid operation mode, FC-battery, the consumed H_2 should be lower than 50 kg/day, and it depends on the energy management strategy recommended by the manufacturer. Considering safety issues and some technical criteria, the tram should be charged after finishing or before starting its daily cycle (from 05:00 till 23:00). Here, it is assumed that the charge of trams is due at 23:00 (at the end of the daily course). All the input parameters are assumed to remain unchanged during the project lifetime. This issue may be discussed in future work.

Fig. 11. Ouargla tramway (in Ouargla city, Algeria), showing its very close proximity to University campus.

16

Energy management strategy (Scenario 2)

In this scenario, the PV system is the first source used to supply the building demand as in the first scenario. However, in this case, the excess electricity generated by PV is solely used by the Ele (as the export of electricity to the grid is not allowed in this case) to produce H_2. The produced H_2 is then stored in the H_2 ST. Besides, when the PV cannot meet the demand, the grid is required to provide such shortage of demand for electricity. In this scenario 2, a sector coupling strategy is applied, in which the stored H_2 in the ST is used to charge FC based trams as described above. Thus, LHSP index is introduced. A flowchart for the energy management strategy applied in scenario 2 is summarized in Fig. 12.
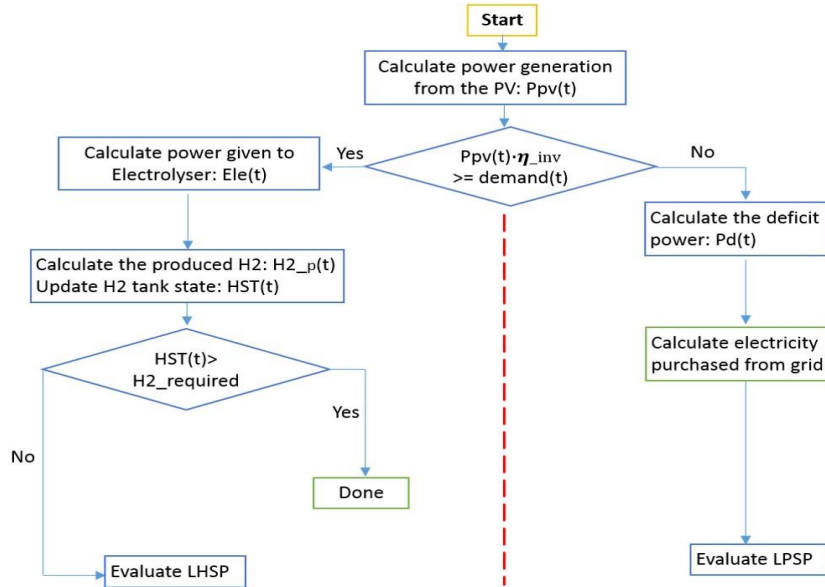
Fig. 12. Flow chart for the energy management using sector coupling strategy (Scenario 2).

In this study, MATLAB software (version 2016b) is used as a platform to simulate the investigated optimization problem, considering the two simulation scenarios described above. First, the mathematical modelling equations for objective functions, constraints and the HRES components are implemented. Furthermore, the suggested energy management strategies and PSO algorithm are written as function files. Thus, climate data (including ambient temperature and solar radiation) and the building load profile for one entire year (8760 hours) are imported. In addition, the technical and economic parameters for the HRES components are also introduced (see, e.g. as shown in Table 2) [36,74]. Within the project lifetime of 20 years, the optimization must proceed until the maximal iteration value is reached. At each time step (one hour) of the simulation, for over 8760 hours of the year, and during the project lifetime, the energy balance between the supply and demand sides is assessed to ensure system reliability. Hence, the objective function, decision variables, and all other considered evaluating criteria are determined. These are presented and discussed in the following section.

Table 2. Techno-economic parameters for the HRES' components.

Generation source	Parameters	Specification
PV	Capital cost ($/kW)	1000
	O&M cost (% of Capital cost)	1
	Temperature coefficient of power (%/°C)	-0.41
	Lifetime (Year)	20
Ele	Capital cost ($/kW)	1000
	O&M cost (% of Capital cost)	1
	Efficiency (%)	80
	Lifetime (Year)	20

17

FC	Capital cost ($/kW)	1500
	Replacement cost ($/kW)	1000
	O&M cost (% of Capital cost)	1%
	Efficiency (%)	60
	Lifetime (year)	10
ST	Capital cost ($/kWh)	10
	O&M cost (% of Capital cost)	1
	Lifetime (year)	20
Converter	Capital/ Replacement cost ($/kW)	200
	Efficiency (%)	95
	Lifetime (Year)	20
Economic parameters	Project lifetime (Year)	20
	i (interest rate) (%)	5

5. Results and Discussion

To test the accuracy of PSO, the obtained results for a baseline case (i.e. the first scenario) are compared with those obtained via the HOMER software. Hereby, the simulation of the scenarios is performed, and the results are presented and discussed as follows.

5.1 Scenario 1

5.1.1 Results of optimal sizing for the proposed HRES

Results of optimal sizing of the HRES for the first scenario are presented in Table 3. In addition, the convergence of the developed code (applying PSO algorithm) for the baseline case simulation is given in Fig. 13, which is in good agreement with that obtained by Samy et al. [34].

Table 3. Result of optimal sizing of the HRES (scenario 1).

Optimizer	HOMER	MATLAB	MATLAB
Maximum value for NRU	NRU^{max}=100%	NRU^{max}=100%	NRU^{max}=1%
Optimal HRES's configuration	PV-grid	PV-grid	PV-grid-FC-ST-Ele
PV [kW]	1916	1916	1916
FC [kW]	0	0	285
Ele [kW]	0	0	616
ST [kWh]	0	0	9857 (equivalent to 296 kg)
LPSP [%]	0	0	0
COE [$/kWh]	0.0154	0.016	0.103
RU [%]	86.4	87	100
CO$_2$ [kg/year]	400409	404339	24307
Energy sold to the grid [MWh/year]	3175	2930	993
Energy purchased from the grid [MWh/year]	633	641	38
Building energy demand [MWh/year]	1486	1486	1486

18

COE ($/kWh)
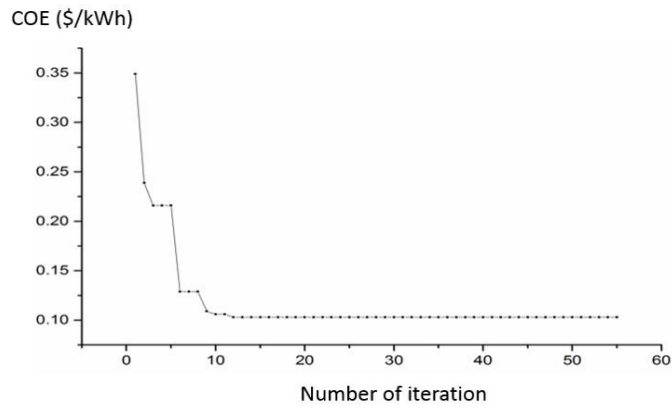
Fig. 13. PSO convergence (with NRU^{max} =1%).

5.1.2 Energy contribution to the HRES components

- In the case of NRU^{max} =100%

The contribution of PV and FC and the energy imported from and exported to the grid are given in Fig. 14.
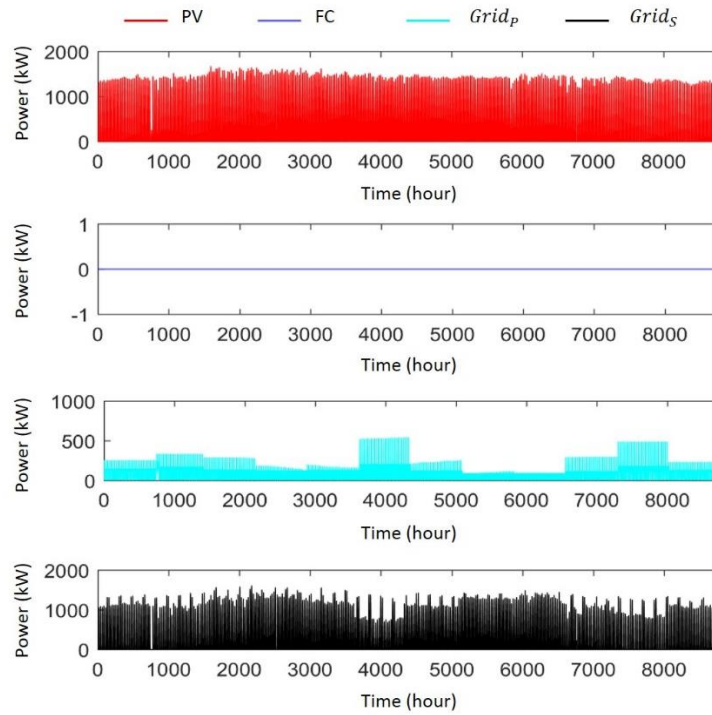
Fig. 14. Energy contribution for the HRES components (NRU^{max} =100%, scenario 1).

- In the case of NRU^{max} =1%

The contributions of PV and FC and the energy imported from and exported to the grid in the case of NRU less than 1% are given in Fig. 15.
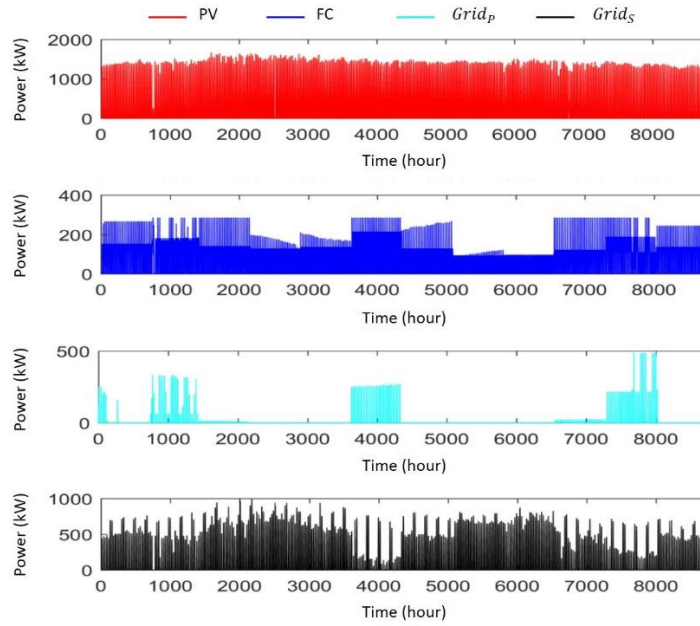
Fig. 15. Energy contribution to the HRES's components (NRU^{max} =1%, Scenario 1).

The obtained results for this scenario 1 show that with NRU^{max}=100%, the best configuration consists of grid and PV system, which fulfils attractive values for COE (0.016 $/kWh) and RU (87%). The H$_2$ is not included in this configuration, because in case of power shortage from the PV (as in the night time), the building prefers to import energy from the grid instead of using FC. This is because the cost of importing energy from the grid is lower than that from FC (which includes the cost of Ele, ST, and FC). In addition, by setting a high value for NRU^{max} (100%), the system is not required to reach high renewable contribution. For this reason, in the second case, a low value of NRU^{max} (1%) is imposed for comparison. In this case, the user prefers a high renewable share (i.e. low CO$_2$ emissions and low import from the grid). Thus, a new optimal configuration is obtained that includes PV, Ele, FC and H$_2$ ST. This HRES configuration reaches RU of 100%, but the obtained COE (0.1 $/kWh) is six times greater than that obtained with a PV-grid system. By comparing the results, it is clear that the grid-connected PV system without H$_2$ is the best configuration for the case study building from an economic point of view and even considering the renewability preferences. Consequently, integrating H$_2$ storage tank to increase HRES reliability is not economically attractive and hard to justify its feasibility in specific countries where low electricity prices exist. For this reason, in this study, a second scenario is suggested which takes into account the requirements of future energy systems, in which a sector coupling strategy is developed and applied to enhance the benefits of HRES-H$_2$ that make them more cost-effective than existing systems.

5.2 Scenario 2

A grid-connected PV system without H$_2$ storage was found to be the best economic solution for the studied building (from scenario 1). However, owing to certain socio-technical barriers (mainly the instability of export electricity from distributed renewable energy systems, the unavailability of feed-in tariffs for building consumers in Algeria until now, and the increasing need for sustainable and clean transportation fuels like H$_2$), an alternative solution, including a sector coupling strategy is suggested in this scenario to overcome the above issues.

5.2.1 Results of optimal sizing for the proposed HRES (scenario 2)
Results of optimal sizing for the HRES under study, according to the second scenario inputs, are given in Table 4.

Table 4. Results of optimal sizing for the proposed HRES (scenario 2).

Number of Trams to be charged	1	2	3	4
PV [kW]	91	903	1281	1608
Ele [kW]	42	589	849	1074
ST [kWh]	264 (8 kg)	5155 (155 kg)	7702 (231 kg)	9100 (273 kg)
LPSP [%]	0	0	0	0
RU [%]	12	71	79	83
LHSP [%]	99	34	26	23
COE [$/kWh]	0.053	0.052	0.046	0.042
CO_2 [kg/year]	832610	455471	424236	411839
Energy purchased from the grid [MWh/year]	1321	722	673	653
H_2_demand [kg/year]	18250	36500	54750	73000
H_2_refueled [kg/year]	184	23937	40787	55952
Building energy demand [MWh/year]	1486	1486	1486	1486

5.2.2 Energy and H_2 contribution by the HRES components

- In the case of one tram charged per day

The contributions of the PV system and the grid in case of integrating one tram per day are presented in Fig. 16. In addition, Fig. 17 shows the refuelled H_2 by the system and the H_2 required by the tram.
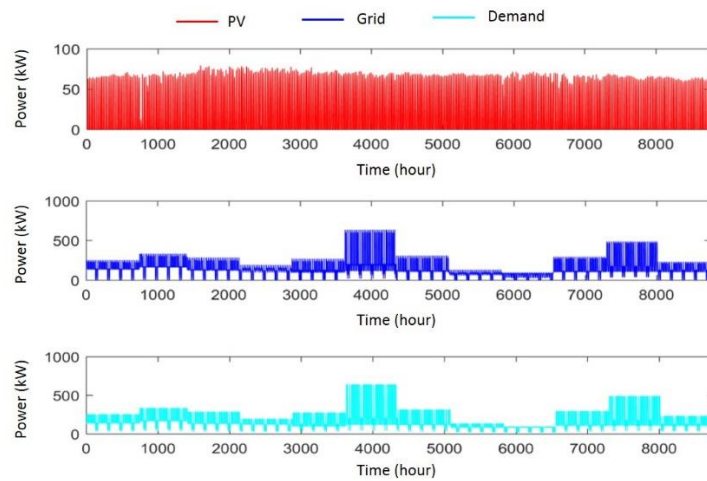
Fig. 16. The contribution of the PV system and the grid (in case of integrating one tram).
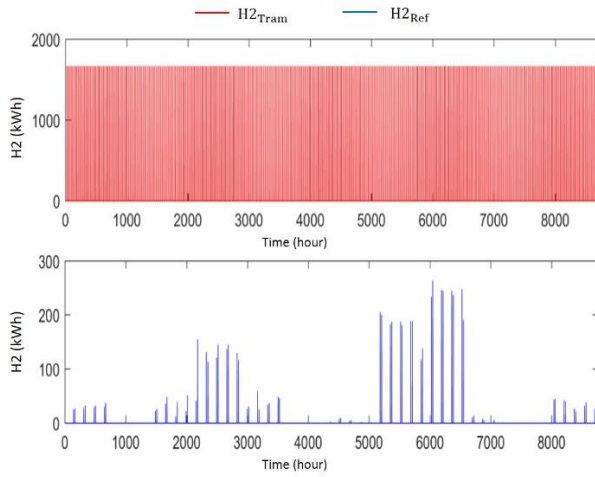
Fig. 17. The refuelled H₂ by the system and the H₂ required by the tram (in case of integrating one tram).

- In the case of three trams charged per day

In the case of three trams to be charged by the studied HRES, the contributions of the PV system and the grid are illustrated in Fig. 18. The refuelled H₂ by the system and the H₂ required by trams are presented in Fig. 19.
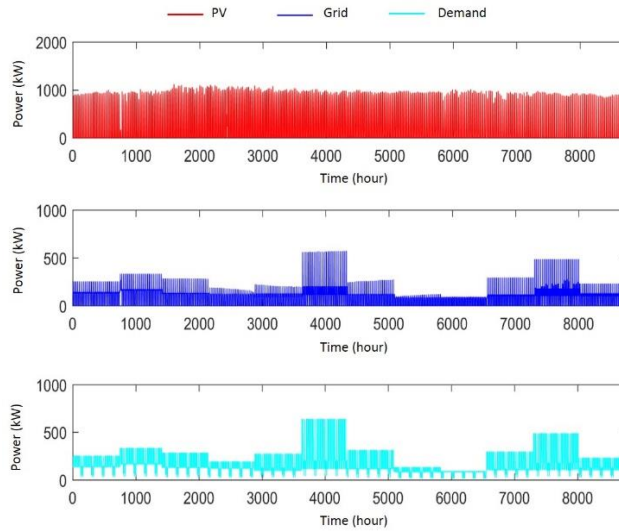
Fig. 18. The contribution of the PV system and the grid (in case of integrating three trams).
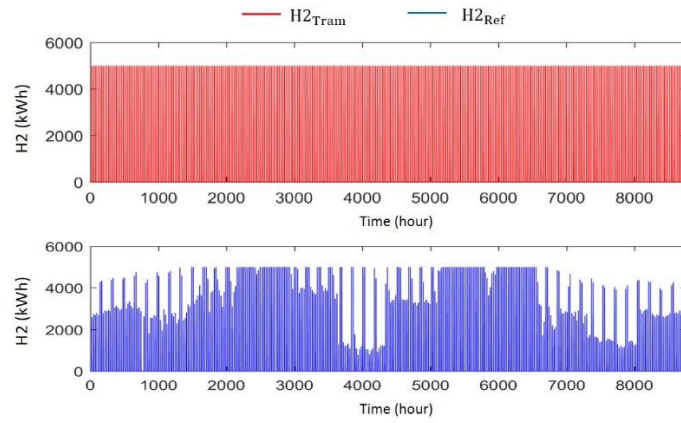
Fig. 19. The refuelled H₂ by the system and the H₂ required by the tram (in case of integrating three trams).

By making a general observation, it is seen that the number of trams to be charged daily (i.e. the daily hydrogen demand by FC trams) has a significant effect on the size optimization of the studied HRES (grid-PV-H₂). Besides, it is observed that the increase in the number of trams (consequently H₂ demands) leads to a reduction in the LHSP, COE, and CO_2 emissions. In contrast, RU is increased. It is noted that with three or more trams, the system can reach grid parity, as the obtained COE (0.046 $/kWh) is less than the electricity purchased from the grid. Within a three tram system integration, the obtained HRES that includes PV (1281 kW), Ele (849 kW) and ST (273 kg) can provide 74% of the H₂ demand (LHSP = 26%) with high RU (79%). As with four trams, the obtained HRES results are similar to those found with three trams, and so it is concluded that the optimal HRES for this scenario is with the one integrating three trams.

The results are associated with the technical and economic feasibility of the proposed grid-connected PV-H₂ hybrid system at the studied University building. The proposed approach allows the consumer to become an energy Prosumer and enables flexible sector coupling, in particular between the building and transportation sector (tram). The outcomes of this study are not only beneficial for the building, but also helpful for the country to make a successful transition towards clean and sustainable energy systems in the future. The application of the proposed method is not only for Algeria alone, but also feasible for any other countries with similar building/transport infrastructure.

6. Conclusions and further work

In this paper, the optimal sizing of a grid-connected HRES including PV, Ele, FC and ST is carried out using PSO based code, for a University building located in the south of Algeria. The proposed HRES is optimized under two scenarios. In the first scenario, the proposed HRES could make power exchange (import/export) with the grid. In the second scenario, a sector coupling strategy is suggested, in which the building can only import the energy from the grid. Besides, it can export the produced H₂ to charge FC trams via an onsite H₂ refuelling station.

The findings can be summarised as follows:
- For the first scenario, it is found that with NRU^{max} =100%, the best configuration is a grid-PV system, which fulfils the grid parity with a lower COE (0.016 $/kWh) and higher RU (87%). By setting NRU^{max} =1%, a hybrid grid-PV-Ele-FC-ST system with an optimized size is the preferred solution. This configuration can achieve 100 % RU but at a higher COE of 0.1 $/kWh, about six times more than that in the first case (NRU^{max} =100%). In both cases, the obtained HRES reaches higher RU. From an economic point of view, it is evident that the grid-connected PV system without H₂ presents the best option for the selected building in this case study.

- For the second scenario, it is seen that the number of trams to be charged daily (i.e. the daily hydrogen required for charging FC trams) has a significant effect on the size optimization of HRES. Specifically, it is observed that the increase in the number of trams (i.e. increased H₂ demand) leads to a reduction in the LHSP, COE, and CO_2 emissions (for the same total runs). However, RU is increased. For example, when accounting for three trams to

be charged, the best HRES configuration includes PV (1281 kW), Ele (849 kW) and ST (273 kg). This configuration provides 74% of the H_2 demand (LHSP is about 26%) and achieves a high RU value (approx. 79%).

Combining the obtained results from both scenarios, it is concluded that:
- Considering economic and renewability preferences, the grid-PV (i.e. the first scenario) system is the best choice for the selected building
- Considering the requirements of future energy systems (where both electricity and H_2 are needed), the grid-connected PV-H_2 (i.e. the second scenario) is the best solution for building/transport sector coupling strategy.

The outcomes of this study show that the suggested sector coupling strategy that was applied to the proposed grid-connected HRES is a promising solution for enabling high renewable usage and for achieving sustainable buildings and cities in Algeria. The investigated building could be an efficient energy prosumer within the proposed energy solution. The findings could help the country make a successful transition from fossil fuel based energy systems to clean and sustainable energy systems. However, further work on how to implement the solution and integrate it within the investigated building is required. In addition, the comparison between the available H_2 storage and transportation technologies (such as pipelines and Liquid Organic H_2 Carrier (LOHC) tanks) will be performed to study the feasibility of connecting such systems with industrial consumers at far away distances.

References

[1]   Zahedi R, Gharehpetian GB. Optimal Sizing of Floating Photovoltaic System Equipped with Hydrogen Tank and Battery ESS. 2019 Smart Gird Conf SGC 2019 2019:1–5. https://doi.org/10.1109/SGC49328.2019.9056632.

[2]   Gouareh A, Settou N, Khalfi A. GIS-based analysis of hydrogen production from geothermal electricity using CO 2 as working fluid in Algeria. Int J Hydrogen Energy 2015;40:15244–53. https://doi.org/10.1016/j.ijhydene.2015.05.105.

[3]   Mokhtara C, Negrou B, Settou N, Gouareh, Abderrahmane BS. Pathways to plus-energy buildings in Algeria : design optimization method based on GIS and multi-criteria decision-making. Energy Procedia 2019;162:171–80. https://doi.org/10.1016/j.egypro.2019.04.019.

[4]   Vimpari J, Junnila S. Estimating the diffusion of rooftop PVs: A real estate economics perspective. Energy 2019;172:1087–97. https://doi.org/10.1016/j.energy.2019.02.049.

[5]   Mellouk L, Ghazi M, Aaroud A, Boulmalf M, Benhaddou D, Zine-dine K. Design and energy management optimization for hybrid renewable energy system- case study : Laayoune region. Renew Energy 2019;139:621–34. https://doi.org/10.1016/j.renene.2019.02.066.

[6]   Abada Z, Bouharkat M. Study of management strategy of energy resources in Algeria. Energy Reports 2018;4:1–6. https://doi.org/10.1016/j.egyr.2017.09.004.

[7]   Government A. Renewable Energy and Energy Efficiency Development Plan 2015-2030. IEA 2015.

[8]   VOSviewer n.d.

[9]   Martinho VJPD. Interrelationships between renewable energy and agricultural economics: An overview. Energy Strateg Rev 2018;22:396–409. https://doi.org/10.1016/j.esr.2018.11.002.

[10]   Phommixay S, Doumbia ML, Lupien St-Pierre D. Review on the cost optimization of microgrids via particle swarm optimization. Int J Energy Environ Eng 2020;11:73–89. https://doi.org/10.1007/s40095-019-00332-1.

[11]   Hou H, Xu T, Wu X, Wang H, Tang A, Chen Y. Optimal capacity configuration of the wind-photovoltaic-storage hybrid power system based on gravity energy storage system. Appl Energy 2020;271:115052. https://doi.org/https://doi.org/10.1016/j.apenergy.2020.115052.

[12] Aberilla JM, Gallego-Schmid A, Stamford L, Azapagic A. Design and environmental sustainability assessment of small-scale off-grid energy systems for remote rural communities. Appl Energy 2020;258:114004. https://doi.org/10.1016/j.apenergy.2019.114004.

[13] Cai W, Li X, Maleki A, Pourfayaz F, Rosen MA, Nazari] M [Alhuyi, et al. Optimal sizing and location based on economic parameters for an off-grid application of a hybrid system with photovoltaic, battery and diesel technology. Energy 2020;201:117480. https://doi.org/https://doi.org/10.1016/j.energy.2020.117480.

[14] Modarresi Ghazvini A, Olamaei J. Optimal sizing of autonomous hybrid PV system with considerations for V2G parking lot as controllable load based on a heuristic optimization algorithm. Sol Energy 2019;184:30–9. https://doi.org/10.1016/j.solener.2019.03.087.

[15] Chedid R, Sawwas A, Fares D. Optimal design of a university campus micro-grid operating under unreliable grid considering PV and battery storage. Energy 2020;200:117510. https://doi.org/https://doi.org/10.1016/j.energy.2020.117510.

[16] Li C, Zhou D, Wang H, Lu Y, Li D. Techno-economic performance study of stand-alone wind/diesel/battery hybrid system with different battery technologies in the cold region of China. Energy 2020;192:116702. https://doi.org/10.1016/j.energy.2019.116702.

[17] Ashraf MA, Liu Z, Alizadeh A, Nojavan S, Jermsittiparsert K, Zhang D. Designing an Optimized Configuration for a Hybrid PV/Diesel/Battery Energy System Based on Metaheuristics: A Case study on Gobi Desert. J Clean Prod 2020:122467. https://doi.org/https://doi.org/10.1016/j.jclepro.2020.122467.

[18] Xu X, Hu W, Cao D, Huang Q, Chen C, Chen Z. Optimized sizing of a standalone PV-wind-hydropower station with pumped-storage installation hybrid energy system. Renew Energy 2020;147:1418–31. https://doi.org/https://doi.org/10.1016/j.renene.2019.09.099.

[19] Berbaoui B, Dehini R, Hatti M. An applied methodology for optimal sizing and placement of hybrid power source in remote area of South Algeria. Renew Energy 2020;146:2785–96. https://doi.org/https://doi.org/10.1016/j.renene.2019.04.011.

[20] Alshammari N, Asumadu J. Optimum unit sizing of hybrid renewable energy system utilizing harmony search, Jaya and particle swarm optimization algorithms. Sustain Cities Soc 2020;60:102255. https://doi.org/https://doi.org/10.1016/j.scs.2020.102255.

[21] Dahiru AT, Tan CW. Optimal sizing and techno-economic analysis of grid-connected nanogrid for tropical climates of the Savannah. Sustain Cities Soc 2020;52:101824. https://doi.org/https://doi.org/10.1016/j.scs.2019.101824.

[22] Mayer MJ, Szilágyi A, Gróf G. Environmental and economic multi-objective optimization of a household level hybrid renewable energy system by genetic algorithm. Appl Energy 2020;269:115058. https://doi.org/https://doi.org/10.1016/j.apenergy.2020.115058.

[23] Habib HUR, Subramaniam U, Waqar A, Farhan BS, Kotb KM, Wang S. Energy cost optimization of hybrid renewables based V2G microgrid considering multi objective function by using artificial bee colony optimization. IEEE Access 2020;8:62076–93. https://doi.org/10.1109/ACCESS.2020.2984537.

[24] Nguyen HT, Safder U, Nhu Nguyen XQ, Yoo CK. Multi-objective decision-making and optimal sizing of a hybrid renewable energy system to meet the dynamic energy demands of a wastewater treatment plant. Energy 2020;191:116570. https://doi.org/10.1016/j.energy.2019.116570.

[25] Jaszczur M, Hassan Q, Palej P, Abdulateef J. optimisation of a micro-grid hybrid Multi-Objectivepower system for household application. Energy 2020;202:117738. https://doi.org/https://doi.org/10.1016/j.energy.2020.117738.

[26] Wang R, Xiong J, He M, Gao L, Wang L. Multi-objective optimal design of hybrid renewable energy system under multiple scenarios. Renew Energy 2020;151:226–37. https://doi.org/https://doi.org/10.1016/j.renene.2019.11.015.

[27] Mokhtara C, Negrou B, Bouferrouk A, Yao Y, Settou N, Ramadan M. Integrated supply–demand energy management for optimal design of off-grid hybrid renewable energy systems for residential electrification in arid climates. Energy Convers Manag 2020;221:113192. https://doi.org/10.1016/j.enconman.2020.113192.

[28] Acar C, Dincer I. The potential role of hydrogen as a sustainable transportation fuel to combat global warming. Int J Hydrogen Energy 2020;45:3396–406. https://doi.org/10.1016/j.ijhydene.2018.10.149.

[29] Aki H, Sugimoto I, Sugai T, Toda M. Optimal operation of a photovoltaic generation-powered hydrogen production system at a hydrogen refueling station Hirohisa. Int J Hydrogen Energy 2018;43:14892–904. https://doi.org/10.1016/j.ijhydene.2018.06.077.

[30] Koponen J, Kosonen A, Ruuskanen V, Huoman K. Control and energy efficiency of PEM water electrolyzers in renewable energy systems Joonas. Int J Hydrogen Energy 2017;2. https://doi.org/10.1016/j.ijhydene.2017.10.056.

[31] Lee M, Hong T, Jeong K, Kim J. A bottom-up approach for estimating the economic potential of the rooftop solar

photovoltaic system considering the spatial and temporal diversity. Appl Energy 2018;232:640–56. https://doi.org/10.1016/j.apenergy.2018.09.176.

[32] Duman AC, Güler Ö. Techno-economic analysis of o ff -grid PV / wind / fuel cell hybrid system combinations with a comparison of regularly and seasonally occupied households. Sustain Cities Soc 2018;42:107–26. https://doi.org/10.1016/j.scs.2018.06.029.

[33] Zhang W, Maleki A, Rosen MA, Liu J. Optimization with a simulated annealing algorithm of a hybrid system for renewable energy including battery and hydrogen storage. Energy 2018;163:191–207. https://doi.org/10.1016/j.energy.2018.08.112.

[34] Samy MM, Barakat S, Ramadan HS. A flower pollination optimization algorithm for an off-grid PV-Fuel cell hybrid renewable system. Int J Hydrogen Energy 2017;44:2141–52. https://doi.org/10.1016/j.ijhydene.2018.05.127.

[35] Jamshidi M, Askarzadeh A. Techno-economic analysis and size optimization of an o ff -grid hybrid photovoltaic , fuel cell and diesel generator system. Sustain Cities Soc 2019;44:310–20. https://doi.org/10.1016/j.scs.2018.10.021.

[36] Jafari M, Armaghan D, Seyed Mahmoudi SM, Chitsaz A. Thermoeconomic analysis of a standalone solar hydrogen system with hybrid energy storage. Int J Hydrogen Energy 2019;44:19614–27. https://doi.org/10.1016/j.ijhydene.2019.05.195.

[37] Samy MM, Barakat S, Ramadan HS. Techno-economic analysis for rustic electrification in Egypt using multi-source renewable energy based on PV/ wind/ FC. Int J Hydrogen Energy 2019;45:11471–83. https://doi.org/10.1016/j.ijhydene.2019.04.038.

[38] Zhang W, Maleki A, Rosen MA, Liu J. Sizing a stand-alone solar-wind-hydrogen energy system using weather forecasting and a hybrid search optimization algorithm. Energy Convers Manag 2019;180:609–21. https://doi.org/10.1016/j.enconman.2018.08.102.

[39] Ghenai C, Salameh T, Merabet A. Technico-economic analysis of off grid solar PV/Fuel cell energy system for residential community in desert region. Int J Hydrogen Energy 2020;45:11460–70. https://doi.org/10.1016/j.ijhydene.2018.05.110.

[40] Mokhtara C., Negrou B., Settou N., Gouareh A., Settou B. CMA, Mokhtara C, Negrou B, Settou N, Gouareh A, Settou B, et al. Decision-making and optimal design of off-grid hybrid renewable energy system for electrification of mobile buildings in Algeria: case study of drilling camps in Adrar. Alger J Env Sc Technol 2020.

[41] Firtina-Ertis I, Acar C, Erturk E. Optimal sizing design of an isolated stand-alone hybrid wind-hydrogen system for a zero-energy house. Appl Energy 2020;274:115244. https://doi.org/10.1016/j.apenergy.2020.115244.

[42] Zhang G, Shi Y, Maleki A, A. Rosen M. Optimal location and size of a grid-independent solar/hydrogen system for rural areas using an efficient heuristic approach. Renew Energy 2020;156:1203–14. https://doi.org/10.1016/j.renene.2020.04.010.

[43] Attemene NS, Agbli KS, Fofana S, Hissel D. Optimal sizing of a wind, fuel cell, electrolyzer, battery and supercapacitor system for off-grid applications. Int J Hydrogen Energy 2020;45:5512–25. https://doi.org/https://doi.org/10.1016/j.ijhydene.2019.05.212.

[44] Haddad A, Ramadan M, Khaled M, Ramadan H, Becherif M. Study of hybrid energy system coupling fuel cell, solar thermal system and photovoltaic cell. Int J Hydrogen Energy 2020;45:13564–74. https://doi.org/10.1016/j.ijhydene.2018.06.019.

[45] Xu C, Ke Y, Li Y, Chu H, Wu Y. Data-driven configuration optimization of an off-grid wind/PV/hydrogen system based on modified NSGA-II and CRITIC-TOPSIS. Energy Convers Manag 2020;215:112892. https://doi.org/10.1016/j.enconman.2020.112892.

[46] Suresh V, M. M, Kiranmayi R. Modelling and optimization of an off-grid hybrid renewable energy system for electrification in a rural areas. Energy Reports 2020;6:594–604. https://doi.org/https://doi.org/10.1016/j.egyr.2020.01.013.

[47] Gutiérrez-Martín F, Calcerrada AB, de Lucas-Consuegra A, Dorado F. Hydrogen storage for off-grid power supply based on solar PV and electrochemical reforming of ethanol-water solutions. Renew Energy 2020;147:639–49. https://doi.org/10.1016/j.renene.2019.09.034.

[48] Abadlia I, Hassaine L, Beddar A, Abdoune F, Bengourina MR. Adaptive fuzzy control with an optimization by using genetic algorithms for grid connected a hybrid photovoltaic–hydrogen generation system. Int J Hydrogen Energy 2020;45:22589–99. https://doi.org/10.1016/j.ijhydene.2020.06.168.

[49] Saleem MS, Abas N, Kalair AR, Rauf S, Haider A, Tahir MS, et al. Design and optimization of hybrid solar-hydrogen generation system using TRNSYS. Int J Hydrogen Energy 2020;45:15814–30. https://doi.org/10.1016/j.ijhydene.2019.05.188.

[50]   Haddad A, Ramadan M, Khaled M, Ramadan HS, Becherif M. Triple hybrid system coupling fuel cell with wind turbine and thermal solar system. Int J Hydrogen Energy 2020;45:11484–91. https://doi.org/10.1016/j.ijhydene.2019.05.143.

[51]   Lin R, Ye Z, Wu B. The application of hydrogen and photovoltaic for reactive power optimization. Int J Hydrogen Energy 2020;45:10280–91. https://doi.org/10.1016/j.ijhydene.2019.08.078.

[52]   Maghami MR, Hassani R, Gomes C, Hizam H, Othman ML, Behmanesh M. Hybrid energy management with respect to a hydrogen energy system and demand response. Int J Hydrogen Energy 2019;45:1499–509. https://doi.org/10.1016/j.ijhydene.2019.10.223.

[53]   Lokar J, Virtič P. The potential for integration of hydrogen for complete energy self-sufficiency in residential buildings with photovoltaic and battery storage systems. Int J Hydrogen Energy 2020. https://doi.org/10.1016/j.ijhydene.2020.04.170.

[54]   You C, Kwon H, Kim J. Economic, environmental, and social impacts of the hydrogen supply system combining wind power and natural gas. Int J Hydrogen Energy 2020. https://doi.org/10.1016/j.ijhydene.2020.06.095.

[55]   Kamel AA, Rezk H, Abdelkareem MA. Enhancing the operation of fuel cell-photovoltaic-battery-supercapacitor renewable system through a hybrid energy management strategy. Int J Hydrogen Energy 2020. https://doi.org/10.1016/j.ijhydene.2020.06.052.

[56]   Marocco P, Ferrero D, Gandiglio M, Ortiz MM, Sundseth K, Lanzini A, et al. A study of the techno-economic feasibility of H2-based energy storage systems in remote areas. Energy Convers Manag 2020;211:112768. https://doi.org/10.1016/j.enconman.2020.112768.

[57]   Gu Y, Chen Q, Xue J, Tang Z, Sun Y, Wu Q. Comparative techno-economic study of solar energy integrated hydrogen supply pathways for hydrogen refueling stations in China. Energy Convers Manag 2020;223. https://doi.org/10.1016/j.enconman.2020.113240.

[58]   Ghaffari A, Askarzadeh A. Design optimization of a hybrid system subject to reliability level and renewable energy penetration. Energy 2020;193:116754. https://doi.org/10.1016/j.energy.2019.116754.

[59]   Rad MAV, Ghasempour R, Rahdan P, Mousavi S, Arastounia M, Vaziri Rad MA, et al. Techno-economic analysis of a hybrid power system based on the cost-effective hydrogen production method for rural electrification, a case study in Iran. Energy 2020;190:116421. https://doi.org/10.1016/j.energy.2019.116421.

[60]   IRENA. Sector coupling 2020.

[61]   Tebibel H, Medjebour R. Comparative performance analysis of a grid connected PV system for hydrogen production using PEM water, methanol and hybrid sulfur electrolysis. Int J Hydrogen Energy 2018;43:3482–98. https://doi.org/10.1016/j.ijhydene.2017.12.084.

[62]   Gharibi M, Askarzadeh A. Size and power exchange optimization of a grid-connected diesel generator-photovoltaic-fuel cell hybrid energy system considering reliability, cost and renewability. Int J Hydrogen Energy 2019;44:25428–41. https://doi.org/10.1016/j.ijhydene.2019.08.007.

[63]   García-Triviño P, Fernández-Ramírez LM, Gil-Mena AJ, Llorens-Iborra F, García-Vázquez CA, Jurado F. Optimized operation combining costs, efficiency and lifetime of a hybrid renewable energy system with energy storage by battery and hydrogen in grid-connected applications. Int J Hydrogen Energy 2016;41:23132–44. https://doi.org/10.1016/j.ijhydene.2016.09.140.

[64]   Singh S, Chauhan P, Singh NJ. Capacity optimization of grid connected solar/fuel cell energy system using hybrid ABC-PSO algorithm. Int J Hydrogen Energy 2020;45:10070–88. https://doi.org/10.1016/j.ijhydene.2020.02.018.

[65]   Darras C, Bastien G, Muselli M, Poggi P, Champel B, Serre-Combe P. Techno-economic analysis of PV/H2 systems. Int J Hydrogen Energy 2015;40:9049–60. https://doi.org/10.1016/j.ijhydene.2015.05.112.

[66]   Kumar A, Singh AR, Deng Y, He X, Kumar P, Bansal RC. Integrated assessment of a sustainable microgrid for a remote village in hilly region. Energy Convers Manag 2019;180:442–72. https://doi.org/10.1016/j.enconman.2018.10.084.

[67]   Wang Y, Wang X, Yu H, Huang Y, Dong H, Qi C. Optimal Design of Integrated Energy System Considering Economics , Autonomy and Carbon Emissions. J Clean Prod 2019. https://doi.org/10.1016/j.jclepro.2019.03.025.

[68]   Maleki A. Design and optimization of autonomous solar-wind-reverse osmosis desalination systems coupling battery and hydrogen energy storage by an improved bee algorithm. Desalination 2018;435:221–34. https://doi.org/10.1016/j.desal.2017.05.034.

[69]   Das BK, Zaman F. Performance analysis of a PV/Diesel hybrid system for a remote area in Bangladesh: Effects of dispatch strategies, batteries, and generator selection. Energy 2019;169:263–76. https://doi.org/10.1016/j.energy.2018.12.014.

[70]   Padrón I, Avila D, Marichal GN, Rodríguez JA. Assessment of Hybrid Renewable Energy Systems to supplied energy to Autonomous Desalination Systems in two islands of the Canary Archipelago. Renew Sustain Energy Rev 2019;101:221–30. https://doi.org/10.1016/j.rser.2018.11.009.

[71]   Negrou B, Settou N, Chennouf N, Dokkar B. Valuation and development of the solar hydrogen production. Int J Hydrogen Energy 2010;36:4110–6. https://doi.org/10.1016/j.ijhydene.2010.09.013.

[72]   Multi-Objective Optimization using Evolutionary Algorithms. PURDUE Univ n.d.

[73]   Twaha S, Ramli MAM. A review of optimization approaches for hybrid distributed energy generation systems : O ff -grid and grid-connected systems. Sustain Cities Soc 2018;41:320–31. https://doi.org/10.1016/j.scs.2018.05.027.

[74]   Fodhil F, Hamidat A, Nadjemi O. Potential , optimization and sensitivity analysis of photovoltaic-diesel-battery hybrid energy system for rural electri fi cation in Algeria. Energy 2019;169:613–24. https://doi.org/10.1016/j.energy.2018.12.049.

[75]   Zahedi R, Ardehali MM. Power management for storage mechanisms including battery, supercapacitor, and hydrogen of autonomous hybrid green power system utilizing multiple optimally-designed fuzzy logic controllers. Energy 2020;204:117935. https://doi.org/10.1016/j.energy.2020.117935.

[76]   Ghorbani N, Kasaeian A, Toopshekan A, Bahrami L. Optimizing a hybrid wind-PV-battery system using GA-PSO and MOPSO for reducing cost and increasing reliability. Energy 2018;154:581–91. https://doi.org/10.1016/j.energy.2017.12.057.

[77]   Liu J, Wu X, Li H, Qi L. An optimal method of the energy consumption for fuel cell hybrid tram. Int J Hydrogen Energy 2020;45:20304–11. https://doi.org/10.1016/j.ijhydene.2019.12.135.

[78]   Watan E. Ouargla Tram n.d.

[79]   Zhang W, Li J, Xu L, Ouyang M, Liu Y, Han Q, et al. Comparison study on life-cycle costs of different trams powered by fuel cell systems and others. Int J Hydrogen Energy 2016;41:16577–91. https://doi.org/10.1016/j.ijhydene.2016.03.032.